Ligand Derivatization of Titanium-functionalized

Polyoxovanadium-alkoxide Clusters

Lauren E. VanGelder, William W. Brennessel, and Ellen M. Matson*

^aDepartment of Chemistry, University of Rochester, Rochester, New York 14627, United States

ABSTRACT.

Alkoxylation of heterometal-functionalized polyoxometalates is an important strategy for tailoring the physical and chemical properties of these multimetallic systems. Here, we describe the targeted synthesis of a series of heterometallic tris-alkoxy functionalized clusters $[Ti_2V_4O_5(OCH_3)_{11}(OCH_2)_3CR'],$ R' CH_3 , where C_2H_5 NO_2 , and $[TiV_5O_6(OCH_3)_{10}(OCH_3)_3CR']$, where R' = C₅H₄N. Product isolation reveals design criteria for the self-assembly of heterometallic POV-alkoxide clusters, and adds further diversity to this family of polyoxometalates.

INTRODUCTION.

Polyoxometalates (POMs) comprise an exceptionally diverse library of inorganic clusters, which have seen applications across disciplines from medicine to materials science. ¹⁻² Consisting of three or more corner- or edge-sharing MO_x (M = V, Mo, W) subunits, POMs form a wide array

of structures, and correspondingly, possess a broad range of optical, electronic, and magnetic properties.²⁻³ Their structural versatility has led to extensive research in functionalization of POMs with organic ligands, serving to both increase the diversity of POM-based structures, and to improve their compatibility with organic media.⁴⁻⁶ Recent years especially have seen an increase in generating POM-based organic-inorganic hybrids *via* covalent grafting of organic moieties to the surface of POMs through ligand substitution at the bridging oxygen atoms.^{1,7} This strategy has proven effective for incorporating of specific functional groups in a predictable and reliable manner, highlighting the promise for future developments of hybrid materials that bridge the gap between organic frameworks and inorganic POM-based clusters.

Incorporation of organic moieties into POM frameworks is not only a viable means for tailoring the properties of these clusters, it is also a common method for increasing the stability of otherwise unstable architectures.^{4, 8} It is this strategy that has made possible the synthesis of hexavanadium-POMs featuring the Lindqvist core $[M_6O_{19}]^{n-2, 8-9}$ While this oxo-bridged structure is well established and readily formed by Mo, W, Nb, and Ta POM assemblies, it is not observed for vanadium, likely due to the high charge that would result from a $[V_6O_{19}]^{8-}$ structure, and the relatively small ionic radius of V^{5+} .^{2, 10} Thus, generation of such hexavanadium systems has only been accomplished by invoking charge compensation *via* ligand substitution at the bridging oxygen atoms. For example, Zubieta *et. al.* have demonstrated this synthetic strategy to great effect, reporting a wide variety of hexavanadium systems featuring trisalkoxy μ -bridging moieties (TRIOLs).^{9, 11-12} While these studies demonstrate the functional group tolerance of the hexavanadium framework, the neutral TRIOL-functionalized oxo-bridged clusters feature exclusively vanadium(V) centers, limiting their redox capabilities to reduction only. This yields electrochemical profiles which typically have only a single accessible redox event.

In 2003, Hartl and coworkers developed a further organic-functionalized Lindqvist POV framework, $[V_6O_7(OR_{12})]$ ($R = CH_3$, C_2H_5). $^{10,\,13-14}$ They discovered that substitution of all twelve bridging oxo units with alkoxide ligands yields a unique structure that contains mixed valent vanadyl ions in its neutral form: $[V^V_2V^{IV}_4O_7(OR)_{12}]^0$. The Robin & Day Class II delocalized electronic structure of this polyoxovanadium-alkoxide (POV-alkoxide) stabilizes *four* reversible redox events (two oxidations and two reductions), enabling the generation of a cationic POM. We have expanded upon this family of homoleptic POV-alkoxides, demonstrating that the bridging - OR group can be extended ($R = C_3H_5$, C_4H_9 , and C_5H_{11}), with retention of the multielectron redox profile observed in the methoxide- and ethoxide-bridged structures. In addition to these homoleptic modifications, our group $^{15-16}$ and others 17 have reported the incorporation of tris-alkoxy (TRIOL) moieties into the POV-alkoxide platform, to generate $[V_6O_7(OR)_9(OCH_2)_3CR']$ ($R = CH_3$, C_2H_5 ;

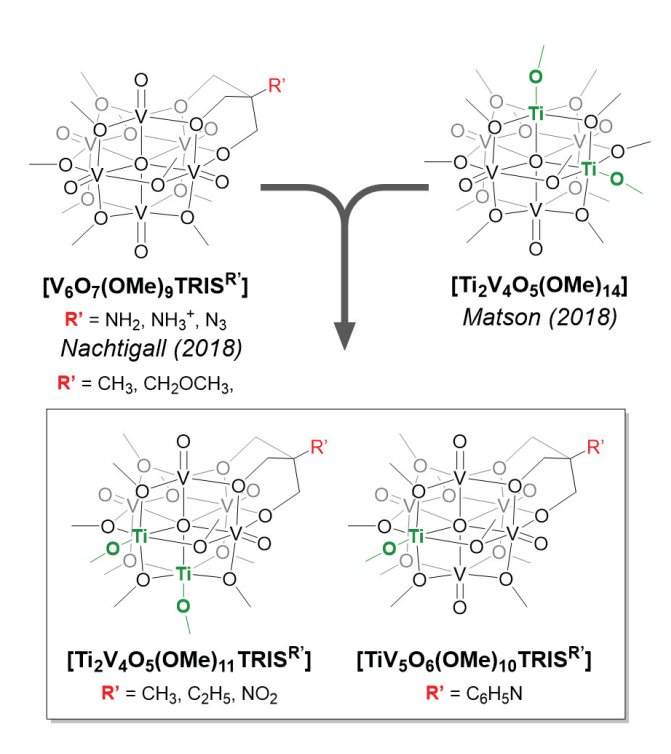


Figure 1. Previously published POV-alkoxide clusters (top) and TRIOL-functionalized heterometallic POV-alkoxides discovered in this work (bottom).

 $R' = NH_2$, N_3 , CH_3 , C_2H_5 , NO_2 , NMe_3^+ , C_5H_4N , $C_5H_5NCH_3$, CH_2OCH_3 , $CH_2OC_2H_4OCH_3$). Each of the clusters in this series feature a single tridentate functional group appended to the face of the cluster, with the nine remaining bridging-alkoxide moieties occupied by methoxide or ethoxide substituents (Figure 1). Notably, as in the case of the homoleptic POV-alkoxides established by Hartl, $[V_6O_7(OR)_{12}]$, these TRIOL-functionalized POV-alkoxides feature a mixed-valent $[V^V_2V^{IV}_4]$ core in their neutral state. This distinguishes these clusters from the previous TRIOL-functionalized POVs, and affords retention of a rich electrochemical profile with four reversible redox events, analogous to the homoleptic POV-alkoxide assemblies. Thus, we conclude that installation of TRIOL ligands is a viable route for incorporating a wide variety of functional groups into POV-alkoxides without impacting their electrochemical properties.

In contrast, we have identified incorporation of transition metal ions into POV-alkoxides as an effective method for tuning the redox properties of this system. We have previously established synthetic routes to generate a series of heterometal functionalized POV-alkoxides, [MV $_5$ O $_6$ (OCH $_3$) $_{12}$] (MV $_5$, where M = Ti, Zr, Hf, Fe, Ga), demonstrating that the heterometal identity has significant bearing on the redox potentials of the V^V/V^{IV} events of the system. ¹⁸⁻²⁰ We also developed routes to access the di-titanium cluster [Ti $_2$ V $_4$ O $_5$ (OCH $_3$) $_1$ 4] (Ti $_2$ V $_4$), discovering that incorporation of a second titanium center yields further shifts in the vanadium-based redox chemistry of the POV-alkoxides and increased stability of the heterometallic Lindqvist core. ²¹ For the titanium-functionalized POV-alkoxides (Ti-POV-alkoxides), TiV $_5$ and Ti $_2$ V $_4$, incorporation of the group(IV) ion results in the appearance of one or two new widely-spaced reduction events in the redox profiles of the mono- and di-titanium clusters, respectively. This distinguishes the Ti-POV-alkoxides from all other heterometallic clusters we have generated, and has made both TiV $_5$

and Ti_2V_4 interesting compounds to consider for electrochemical applications, such as stationary energy storage.²²

Here, we continue to probe the electronic participation of titanium in the hexametalate core through the synthesis and characterization of TRIOL-functionalized Ti-POV-alkoxides. We functional investigate variety of groups the TRIOL ligand, generating at $[Ti_2V_4O_5(OCH_3)_{11}(OCH_2)_3CR'],$ where R' CH₃. C_2H_5 NO_2 and [TiV₅O₆(OCH₃)₁₀(OCH₃)₃CC₅H₄N]. In isolating these complexes, we identify how ligand identity can influence self-assembly, and develop strategies for generating pure products from solvothermal syntheses. Electrochemical analysis reveals consistent electrochemical profiles of the heterometallic Lindqvist clusters, featuring both titanium- and vanadium-based redox events despite variation in functional group identity on the TRIOL ligand. These investigations further highlight the modularity of the POV-alkoxide scaffold, and serve as an example of successful targeted self-assembly. The synthetic insights herein inform strategies for further derivatization of POV-alkoxides, enabling diversification of POM-based organic-inorganic hybrids.

RESULTS AND DISCUSSION.

Synthesis of TRIOL-functionalized Ti-POV-alkoxides.

In our previous work investigating titanium functionalization of POV-alkoxides, we discovered that small variations in solvothermal conditions would favor installation of one or two titanium centers during self-assembly. 18,21 Of the two, the di-titanium cluster, Ti_2V_4 is seemingly the thermodynamically preferred product, as the complex forms directly from solvothermal reaction of the titanium- and vanadium-alkoxide precursors, $Ti(OCH_3)_4$ and $VO(OCH_3)_3$, in

methanol and elevated temperatures and extended reaction times. We note in this synthesis that 48 hours marks the earliest time that Ti_2V_4 is the exclusive product of the reaction, but that heating can continue for up to 120 hours with no impact on product formation. In contrast, installation of a single titanium center to form TiV_5 requires milder reaction conditions. The same titanium and vanadium-alkoxide precursors are used, in 1:5 ratio in methanol, but also necessary for self-assembly is the addition of an external reductant, tetrabutylammonium borohydride [nBu_4N][BH4]. Heating of this reaction is limited to 100 oC for 24 hours, as increased temperature or time results in the formation of significant amounts of Ti_2V_4 . Even under these reaction conditions, purification of TiV_5 still requires extensive washing to remove the byproduct, Ti_2V_4 . Given the additional challenges posed by isolation of the mono-titanium clusters, we narrowed our initial synthetic targets to TRIOL functionalized derivatives of the di-titanium POV-alkoxide, to yield $[Ti_2V_4O_5(OCH_3)_{11}(OCH_2)_3CR^*)$].

We initiated efforts to generate TRIOL-functionalized di-titanium POV-alkoxides beginning with the simplest, commercially available tris-alkoxy precursor, $(HOCH_2)_3CCH_3$ (TRIS^{Me}). Synthetic strategies invoked insights from both our previous work in synthesizing TRIOL-functionalized POV-methoxide clusters¹⁶ as well as our synthetic protocols for generating the di-titanium cluster Ti_2V4 .²¹ The solvothermal reaction of the TRIS^{Me} precursor (one equiv) with the titanium-alkoxide $Ti(O^iPr)_4$ and the vanadium(V) oxytris-methoxide precursor $VO(OCH_3)_3$ (2 and 4 equivalents, respectively) in methanol at 125 °C for 48 hours resulted in the desired Lindqvist cluster $[Ti_2V_4O_5(OCH_3)_{11}(OCH_2)_3CCH_3]$ ($Ti_2V_4TRIS^{Me}$), as indicated by electrospray ionization mass spectrometry (ESI-MS; Figure S1). However, these reaction conditions also gave a small amount of the homoleptic cluster, Ti_2V_4 (m/z = 814), shown in the ESI-MS of the crude reaction (Figure S1). To minimize this byproduct, a slight excess of TRIS^{Me}

was used (1.5 equiv) which shifted product formation to exclusively $Ti_2V_4TRIS^{Me}$, as determined by ESI-MS (Figure S2, Scheme 1). We note that a small excess is also required for clean formation of the analogous hexavanadium-TRIS^{Me} complex [V₆O₇(OCH₃)₉(OCH₂)₃CCH₃] (1.2 equiv TRIS^{Me}/cluster).¹⁶

2
$$Ti(O^{i}Pr)_{4} + 4 VO(OMe)_{3}$$

+

HO

1.5 HO

R

[$Ti_{2}V_{4}O_{5}(OMe)_{11}TRIS^{R}$]

R = -CH₃ ($Ti_{2}V_{4}$ -TRIS^{Me})

-C₂H₅ ($Ti_{2}V_{4}$ -TRIS^{NO2})

Scheme 1. Synthesis of Ti_2V_4 -TRIS^{Me}, Ti_2V_4 -TRIS^E, and Ti_2V_4 -TRIS^{NO}2

Analogous reaction conditions were used to access [Ti₂V₄O₅(OCH₃)₁₁(OCH₂)₃CR'], R' = C₂H₅ (Ti₂V₄TRIS^{Et}), R' = NO₂ (Ti₂V₄-TRIS^{NO₂}), whose formation was likewise indicated by ESI-MS of the crude solutions (Figures S3 and S4). For each reaction, analytically pure material was obtained *via* precipitation of solid from the crude mother liquor. After solutions were left to stand overnight, a microcrystalline, spherulites was observed (Figure S5). Characterization of these solids *via* ¹H NMR reveals three paramagnetic peaks, bearing similarities to the spectrum reported for complex Ti₂V₄ (Figure S6). Infrared spectroscopy was used to further confirm the formation of each desired Lindqvist species, Ti₂V₄-TRIS^{Me}, Ti₂V₄-TRIS^{Et}, and Ti₂V₄-TRIS^{NO₂}.

In the spectra for each cluster, two strong absorption bands are observed at ~975 and ~1020 cm⁻¹, corresponding to the $\nu(V=O_t)$ (O_t = terminal oxo) and $\nu(O_b-CH_3)$ (O_b = bridging oxo), respectively (Figure 2a, Table 1). Additionally, the IR spectra of each TRIOL-functionalized di-titanium cluster show strong absorption bands at ~1125 cm⁻¹, consistent with the $\nu(O-CH_3)$ of the alkoxide ligands bound to the heterometallic titanium centers. Analogous features have been observed in the IR spectrum of the homoleptic cluster Ti_2V_4 . The spectrum of Ti_2V_4 - $TRIS^{NO_2}$ also features two strong absorption bands at 1124 and 1339 cm⁻¹, consistent with the N-O stretching frequencies of the nitro group on the cluster.

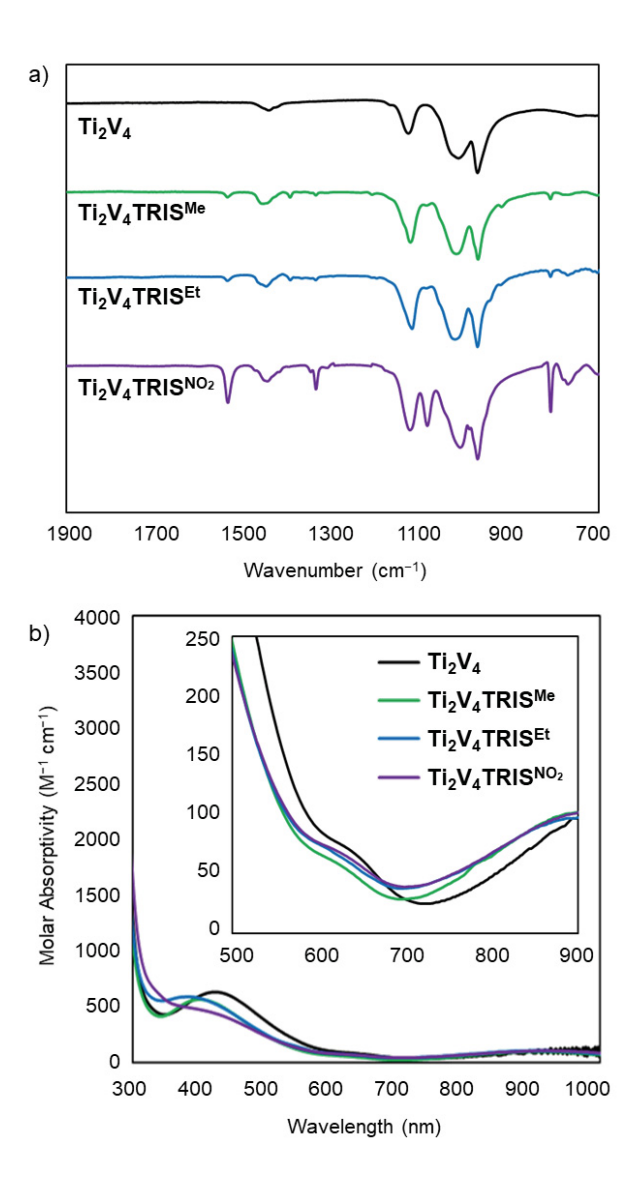


Figure 2. Spectroscopic characterization of Ti₂V₄, Ti₂V₄-TRIS^{Me}, Ti₂V₄-TRIS^{Et}, and Ti₂V₄-TRIS^{NO}₂. (a) IR spectra and (b) electronic absorption spectra collected in acetonitrile. The inset shows the low-energy region of the spectra to more clearly illustrate IVCT bands.

 $\label{eq:table 1.} Table 1. \ \ IR \ \ data \ for \ complexes \ Ti_2V_4, \ Ti_2V_4-TRIS^{Me}, \ Ti_2V_4-TRIS^{Et}, \ Ti_2V_4-TRIS^{NO_2}, \ TiV_5, \\ and \ TiV_5-TRIS^{Py}$

Complex	$v(V=O_t) \text{ cm}^{-1}$	$v(O_b-CH_3) \text{ cm}^{-1}$	v(TiO-CH ₃) cm ⁻¹	v(N-O) cm ⁻¹
Ti ₂ V ₄ ²¹	979	1032	1130	
Ti_2V_4 - $TRIS^{Me}$	972	1018	1124	
$Ti_{2}V_{4}\text{-}TRIS^{Et}$	974	1022	1120	
Ti_2V_4 -TRIS NO_2	974	1013	1124	1124, 1339
TiV ₅ 18	958	1040	1152	
TiV ₅ -TRIS ^{Py}	958	1036	1162	

Further characterization of the cluster core was obtained using electronic absorption spectroscopy. Mixed-valent POV-alkoxide clusters exhibit intervalence charge-transfer (IVCT) bands characteristic of electron transfer between V^{IV} (d^I) centers and V^V (d^0) centers. $^{14,22-24}$ These features are absent in the spectra of Ti_2V_4 - $TRIS^{Me}$, Ti_2V_4 - $TRIS^{Et}$, and Ti_2V_4 - $TRIS^{NO_2}$, suggesting that these clusters possess, instead, an isovalent, V^{IV} electron configuration (Figure 2b). This is analogous to the observations made for the neutral, homoleptic cluster Ti_2V_4 , 21 suggesting that Ti_2V_4 - $TRIS^{Me}$, Ti_2V_4 - $TRIS^{Et}$, and Ti_2V_4 - $TRIS^{NO_2}$ have the same electron configuration of $[Ti^{IV}_2V^{IV}_4]$. This oxidation state distribution is further confirmed by the presence of a weak shoulder around 630 nm (\sim 70 M⁻¹ cm⁻¹), a feature observed in Ti_2V_4 (684 nm, 117 M⁻¹ cm⁻¹), as well as in the di-anionic hexavanadium cluster $[V^{IV}_6O_7(OCH_3)_{12}]^{2-}$ (630 nm, 50 M⁻¹ cm⁻¹). 14,24 Also noted in the spectra of each di-titanium cluster is a broad absorbance around 420 nm,

corresponding to electron transfer between $V^{IV}\left(d^{l}\right)$ to $Ti^{IV}\left(d^{0}\right)$ ions within the heterometallic clusters. 18, 21-22

To unambiguously confirm their structures, crystals of Ti₂V₄-TRIS^{Et} and Ti₂V₄-TRIS^{NO₂} were grown from saturated methanol solution and slow evaporation of dichloromethane, respectively. Refinement of the X-ray data revealed the expected di-titanium Lindqvist structure with three bridging-methoxides replaced by the respective tris-alkoxy functional group (Figure 3, Table 2). The overall cluster geometry closely resembles that of the homoleptic Ti₂V₄, with the two titanium centers located "cis" to one another, linked by a bridging-methoxide unit. As in Ti₂V₄, the Ti-O_m-C bond angles (O_m = oxygen atom of the terminal methoxide ligand) of the capping methoxides for both titanium centers in Ti₂V₄-TRIS^{Et} and Ti₂V₄-TRIS^{NO}₂ are nearly linear (~175 °), with short Ti-O_m bond distances of ~1.75 Å. This suggests significant π -donation from the oxygen atoms of the methoxide moieties to the electron deficient titanium centers. The Ti-O_c (O_c = central μ ^ooxvgen atom) bond distances of Ti₂V₄-TRIS^{Et} and Ti₂V₄-TRIS^{NO}₂ are relatively short (~2.100 and ~2.127 Å) compared to the V_t-O_c bond lengths in each cluster (~2.501 and ~2.472 Å, respectively; V_t = vanadium center located "trans" to the two titanium centers). As in the case of Ti_2V_4 , the affinity of the titanium ions for the μ^6 -oxo seemingly pulls the oxygen atom out of its central position in the cluster, as evidenced by elongated V_t-O_c bond distances. We note that in both Ti₂V₄-TRIS^{Et} and Ti₂V₄-TRIS^{NO}₂ the TRIS^R ligand is bound exclusively to oxygen atoms that bridge two vanadium centers.

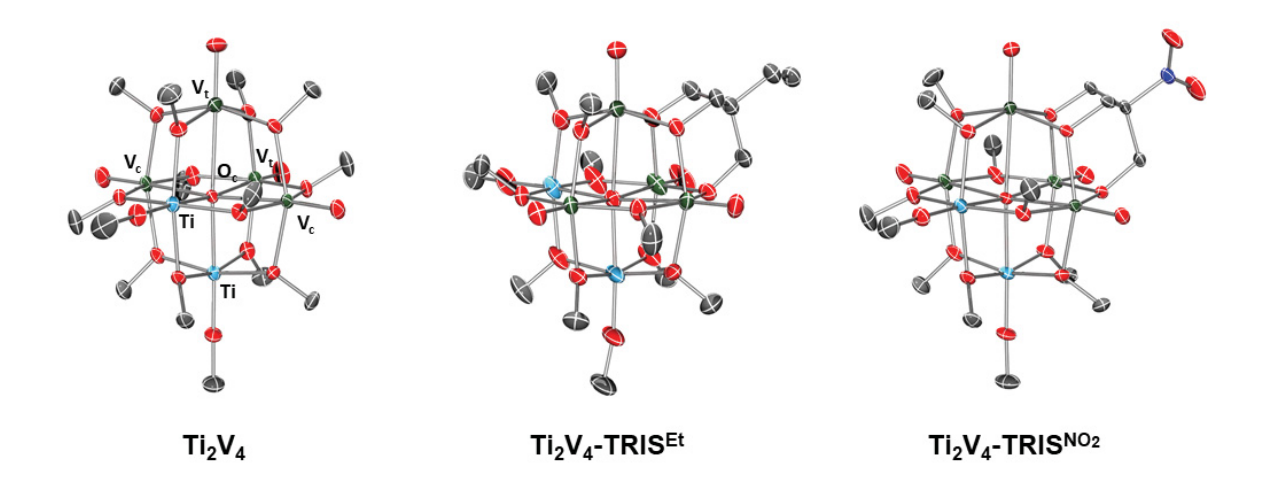


Figure 3. Molecular structure of Ti_2V_4 , Ti_2V_4 - $TRIS^{EL}$, and Ti_2V_4 - $TRIS^{NO_2}$ shown with 50% probability ellipsoids. Hydrogen atoms have been removed for clarity.

Table 2. Structural parameters of Ti_2V_4 , Ti_2V_4 -TRIS et, and Ti_2V_4 -TRIS NO_2

Bond	Ti ₂ V ₄	Ti ₂ V ₄ -TRIS ^{Et}	Ti ₂ V ₄ -TRIS ^{NO} ₂
Ti-O _m (avg)	1.742 Å	1.750 Å	1.745 Å
Ti-O _m -C (avg)	177.6 °	172.9 °	177.3 °
Ti-O _b (avg)	1.976 Å	1.975 Å	1.973 Å
Ti-O _c (avg)	2.126 Å	2.100 Å	2.127 Å
$V-O_t(avg)$	1.601 Å	1.598 Å	1.597 Å
V _t -O _c (avg)	2.473 Å	2.501 Å	2.472 Å
V _c -O _c (avg)	2.373 Å	2.364 Å	2.358 Å

 O_m = oxygen atom of the terminal methoxide ligand; O_b = oxygen atom of the bridging methoxide ligands; O_c = central μ^o -oxygen atom; V_c = vanadium centers "trans" to the titanium atoms; V_c = vanadium centers "cis" to the titanium atoms.

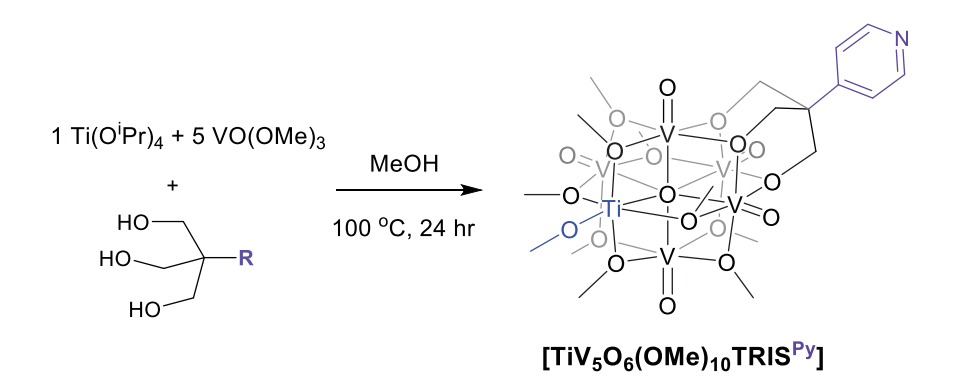
Interested in using TRIOL functionalization as a route for exploring post-synthetic modifications to the POV-alkoxide scaffold, we sought to functionalize the di-titanium cluster with a pyridyl-terminated tris-alkoxy ligand, to generate $[Ti_2V_4O_5(OCH_3)_2(OCH_2)_3CC_5H_4N]$ (Ti₂V₄-

TRIS^{Py}). We have recently demonstrated that the TRIS^{Py} ligand can be successfully incorporated into the mixed-valent, hexavanadium POV-alkoxide framework,¹⁵ and so we hypothesized that incorporation into the di-titanium system would be similarly straightforward. For the homometallic, hexavanadium system, installation of a TRIS^{Py} moiety follows the same synthetic pathway as functionalization with TRIS^{Et} or TRIS^{NO2}. As such, we initiated synthetic efforts to isolate Ti₂V₄-TRIS^{Py} using analogous syntheses to those described for Ti₂V₄-TRIS^{Me}, Ti₂V₄-TRIS^{Et}, and Ti₂V₄-TRIS^{NO2}.

However, following the 48 hour solvothermal reaction (125 °C) of two equiv of Ti(OⁱPr)₄ with four VO(OCH₃)₃ and 1.5 TRIS^{Py} in methanol, ESI-MS revealed that only a small fraction of resulting reaction mixture contained the desired product Ti_2V_4 -TRIS^{Py} (m/z = 902; Figure S7a). Instead, the major species detected via mass spectrometry corresponds to the formation of the TRIS^{Py}-functionalized *mono*-titanium cluster, [TiV₅O₆(OCH₃)₁₀(OCH₂)₃CC₅H₄N] (**TiV₅-TRIS**^{Py}; m/z = 890). Given that formation of the mono-titanium cluster TiV₅ is facilitated by the addition of reductant, [ⁿBu₄N][BH₄], to the solvothermal reaction, we hypothesized that the reducing nature of the pyridyl functional group in the TRIS^{Py} ligand was the cause for the observed product distribution. Yet lowering the amount of TRIS^{Py} added (from 1.5 to 1 equiv) yielded a nearly identical product distribution, with the majority product still TiV₅-TRIS^{Py} (Figure S7b). Our initial syntheses of TiV₅ and Ti₂V₄ revealed that formation of the di-titanium cluster is increasingly favored as the duration of the reaction increases (with exclusive formation at $t \ge 48$ hours). As such, we increased the duration of the aforementioned solvothermal synthesis from 48 to 72 hours, in hopes that we would see an analogous shift in product formation toward the desired di-titanium complex Ti₂V₄-TRIS^{Py}. However, despite variation of reaction conditions we observe no significant change in the ratio of Ti₂V₄-TRIS^{Py} to TiV₅-TRIS^{Py}, but instead the formation of the

homoleptic complex, Ti₂V₄ (Figure S7c). Further increase in reaction time to 96 hours yields exclusive formation of Ti₂V₄ (Figure S7d).

Given the observed preference for its formation, we shifted our target to isolation of the mono-titanium complex TiV_5 - $TRIS^{Py}$. To avoid formation of Ti_2V_4 - $TRIS^{Py}$, we reduced both the duration and temperature of the solvothermal synthesis (from 125 °C for 48 hr to 100 °C for 24 hr), to ideally promote exclusive formation of TiV_5 - $TRIS^{Py}$ (Scheme 2). ESI-MS (-ve) of the resulting green-brown solution revealed a single peak at m/z = 890, corresponding to the exclusive formation of TiV_5 - $TRIS^{Py}$ (Figure S8). Upon standing overnight, a sticky green-brown solid precipitated from the solution. Elemental analysis of this precipitate matched that of the desired product TiV_5 - $TRIS^{Py}$ (EA calculated for $C_{19}H_{40}NO_{19}TiV_5$ (MW=890 g/mol): C, 25.67; H, 4.53; N, 1.58. Found: C, 25.601; H, 4.400; N, 1.438).



Scheme 2. Synthesis of TiV₅-TRIS^{Py}

Characterization of **TiV**₅-**TRIS**^{Py} *via* IR, and absorption spectroscopies confirms formation of the heterometallic cluster core (Table 1). The IR spectrum of **TiV**₅-**TRIS**^{Py} possesses the characteristic V=O_t and O_b-CH₃ stretching frequencies at 958 and 1036 cm⁻¹, respectively, in addition to the TiO-CH₃ stretching frequency observed for all Ti-POVs (1162 cm⁻¹; Figure 4a).¹⁸,

The electronic absorption spectrum of the cluster bears two strong absorbance at 382 and 1000 nm (4.29 x 10^3 and 7.65 x 10^2 M⁻¹ cm⁻¹, respectively), features well established to correspond to intervalence charge-transfer from V^{IV} to V^V centers in POV-alkoxide clusters (Figure 4b).^{14, 19, 23} While such features are not observed in the absorption spectrum of the originally reported, monotitanium functionalized POV-alkoxide cluster in its anionic, reduced state, $[Ti^{IV}V^{IV}{}_5O_6(OCH_3){}_{13}]^-$ (TiV₅), they have been reported for the singly oxidized cluster in a neutral charge state, $[Ti^{IV}V^{V}{}_1V^{V}{}_4O_6(OCH_3){}_{13}]$ (Figure 4b). Thus, we conclude that the electronic distribution of the hexametalate core of TiV₅-TRIS^{Py} directly accessed from solvothermal synthesis is $[Ti^{IV}V^{V}{}_1V^{IV}{}_4]$, with the overall cluster bearing a neutral charge.

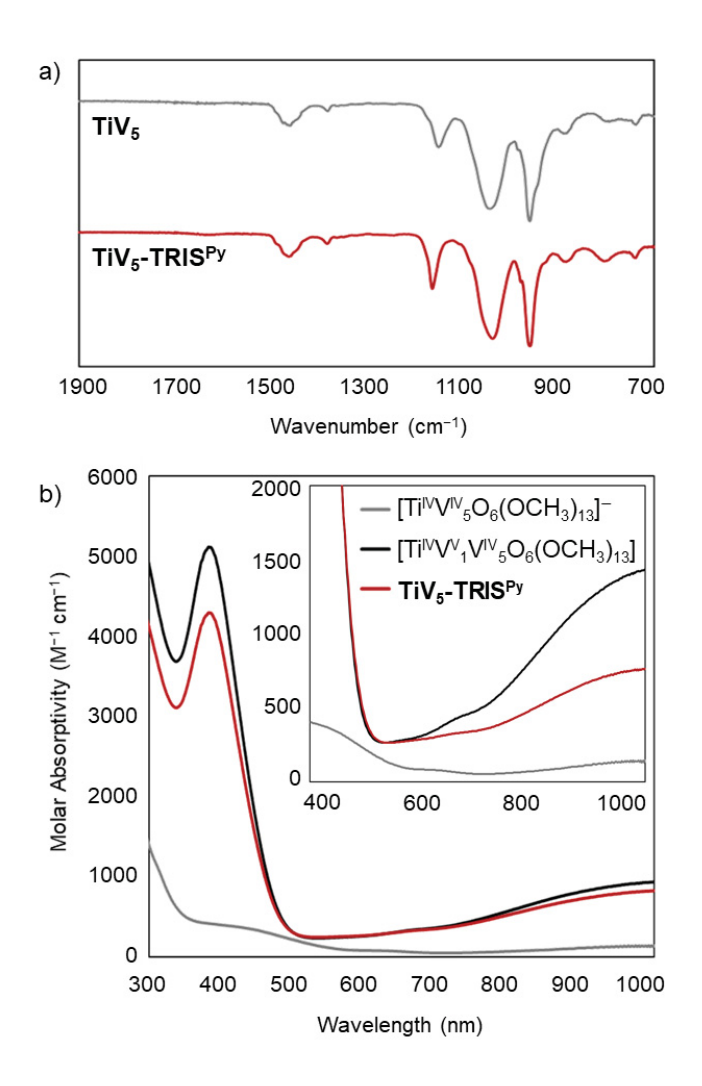


Figure 4. Spectroscopic characterization of TiV_5 - $TRIS^{Py}$, $[Ti^{IV}V^{IV}_5O_6(OCH_3)_{13}]^-(TiV_5)$, and $[Ti^{IV}V^V_1V^{IV}_4O_6(OCH_3)_{13}]$ (a) IR spectra and (b) electronic absorption spectra collected in acetonitrile. The inset shows the low-energy region of the spectra to more clearly illustrate IVCT bands.

Electronic properties of TRIOL-functionalized Ti-POV-alkoxides.

Electrochemical analysis of the series of newly synthesized TRIOL-functionalized Ti-POV-alkoxides was performed *via* cyclic voltammetry (CV). All electrochemical experiments

were run in acetonitrile with tetrabutylammonium hexafluorophosphate ([ⁿBu₄N][PF₆]) as the supporting electrolyte. In each voltammogram four quasi-reversible electrochemical events are observed, analogous to the homoleptic cluster Ti₂V₄ (Figure 5, Table 3). As such, we conclude that the two reduction events in each spectrum ($E_{1/2} \approx -1.6$, -2.1 V) correspond to Ti^{IV}/Ti^{III} redox couples, while the two oxidation events ($E_{1/2} \approx 0.2, 0.7 \text{ V}$) correspond to V^V/V^{IV} couples. We note that across the series of triol-functionalized Ti-POVs, the most reducing $\mathrm{Ti^{IV}/Ti^{III}}$ couple ($E_{1/2} \approx$ -2.1 V) appears less reversible than it does in the homoleptic Ti₂V₄. This may be due to reduced diffusion or kinetics rates in the bulkier functionalized species, though no such losses are observed for the TRIOL-functionalized hexavanadium POV-alkoxides. 15-16 It may also be that TRIOLfunctionalization influences the extent of delocalization within the hexametalate core, and the effects of this are simply most pronounced at this highly reducing event. The $E_{1/2}$ values for each redox event in Ti₂V₄-TRIS^{Ne}, Ti₂V₄-TRIS^E compare favorably with those observed in the spectrum of Ti₂V₄, showing only slight deviations from their homoleptic congener. In contrast the redox events in Ti_2V_4 - $TRIS^{NO_2}$ are significantly shifted, with the V^V/V^{IV} and Ti^{IV}/Ti^{III} couples at potentials ~0.33 V and ~0.11 V higher, respectively, than those in Ti₂V₄. These observations are analogous to those made for the hexavanadium TRIOL-functionalized POV-alkoxide series $[V_6O_7(OC_2H_5)_9TRIS^R]$ (R = -CH₃, -NO₂), wherein the V^V/V^{IV} couples of the R = NO₂ cluster are oxidatively shifted by ~ 0.2 V, while for R = CH₃ no shifts are observed. We hypothesize that, as in the case of the hexavanadium systems, the electron-withdrawing nature of NO₂ influences the redox properties of the POV-alkoxides significantly more than the relatively inert methyl or ethyl substituents.

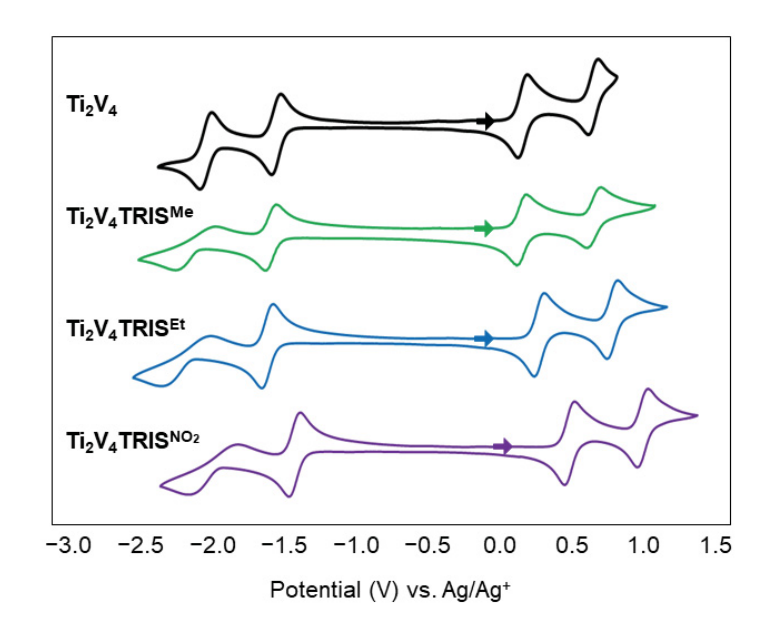


Figure 5. Cyclic voltammograms of Ti_2V_4 , Ti_2V_4 - $TRIS^{Me}$, Ti_2V_4 - $TRIS^{Et}$, and Ti_2V_4 - $TRIS^{NO_2}$ recorded in acetonitrile with 0.1 M [nBu_4][PF₆]. Scan rate 100 mV/s. Arrow indicates open circuit potential and sweep direction.

 $Table~3.~ \mbox{Electrochemical parameters for}~Ti_2V_4, Ti_2V_4-TRIS^{Me}, Ti_2V_4-TRIS^{Et}, \mbox{ and } Ti_2V_4-TRIS^{NO}_2$

	$Ti^{\text{III}}_{2}/Ti^{\text{III}}Ti^{\text{IV}}$	$Ti^{\text{\tiny III}}Ti^{\text{\tiny IV}}/Ti^{\text{\tiny IV}}_{2}$	$\mathbf{V}^{\text{IV}}_{4}/\mathbf{V}^{\text{V}}_{1}\mathbf{V}^{\text{IV}}_{3}$	$V_{\scriptscriptstyle 1}^{\scriptscriptstyle V}V_{\scriptscriptstyle 1}^{\scriptscriptstyle IV}/V_{\scriptscriptstyle 2}^{\scriptscriptstyle V}V_{\scriptscriptstyle 2}^{\scriptscriptstyle IV}$
Ti ₂ V ₄	-2.10	-1.58	0.15	0.64
$Ti_{2}V_{4}\text{-}TRIS^{Me}$	-2.12	-1.60	0.14	0.65
$Ti_{2}V_{4}\text{-}TRIS^{Et}$	-2.21	-1.63	0.26	0.77
Ti_2V_4 - $TRIS^{NO_2}$	-2.01	-1.45	0.47	0.98

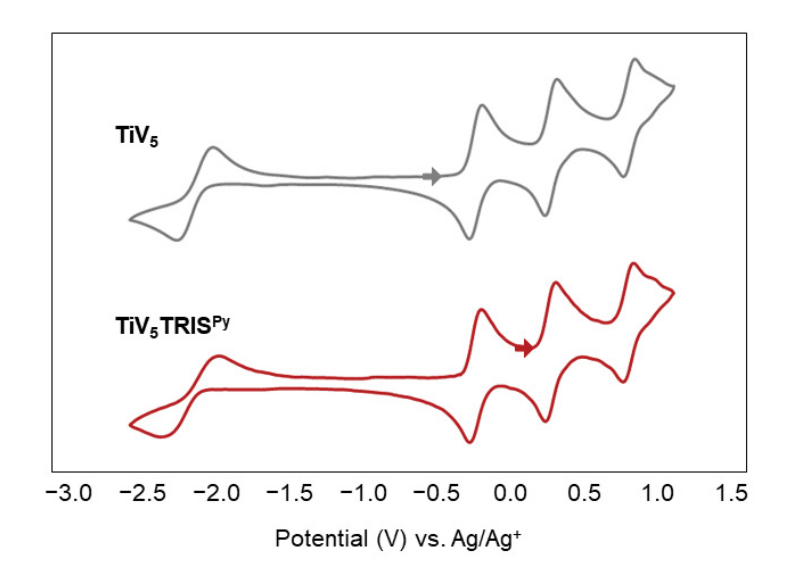


Figure 6. Cyclic voltammograms of **TiV**₅ and **TiV**₅-**TRIS**^{Py} recorded in acetonitrile with 0.1 M [ⁿBu₄][PF₆]. Scan rate 100 mV/s. Arrow indicates open circuit potential and sweep direction.

Table 4. Electrochemical parameters for TiV₅ and TiV₅-TRIS^{Py}

	Ti ^m /Ti ^r	$V_{\scriptscriptstyle \text{IV}}/V_{\scriptscriptstyle 1}V_{\scriptscriptstyle 1}$	$V_{\scriptscriptstyle 1}^{\scriptscriptstyle V}V_{\scriptscriptstyle 1}^{\scriptscriptstyle IV}\!/V_{\scriptscriptstyle 2}^{\scriptscriptstyle V}V_{\scriptscriptstyle 1}^{\scriptscriptstyle IV}$	$V_{2}^{v}V_{3}^{rv}/V_{3}^{v}V_{3}^{rv}$
TiV ₅	-2.07	-0.23	0.24	0.75
TiV ₅ -TRIS ^{Py}	-2.13	-0.25	0.24	0.74

The CV of TiV_5 - $TRIS^{Py}$ is nearly identical to that of the homoleptic TiV_5 , bearing four events at $E_{1/2} = -2.13$, -0.25, 0.24, and 0.74 V (Figure 6, Table 4). Thus, we can correlate the event at -2.13 V to a Ti^{IV}/Ti^{III} reduction, while the three remaining events correspond to V^V/V^{IV} couples. We note that unlike the anionic, isovalent V^{IV} cluster, TiV_5 , which has an open circuit potential (OCP) of -0.5 V, the OCP of TiV_5 - $TRIS^{Py}$ is 0.2 V, further evidence of the mixed-valent $V^{V_1}V^{IV_4}$ core of the cluster isolated directly from solvothermal synthesis. In our previous work

with the hexametalate system [V₆O₇(OC₂H₅)₉TRIS^{Py}], we observed a slight shift (+0.1 V) upon tris-pyridyl functionalization.¹⁵ Although this is more significant than the changes in redox profile observed here upon tris-pyridyl functionalization of the mono-titanium cluster (which are effectively non-existent), the electrochemical changes in both cases can be comparably classified as minimal.

Overall, we conclude that the shifts imparted to the POV-alkoxide series by ligand identity are much smaller than those observed for functionalized oxo-bridged POVs. For example, in the TRIOL-functionalized POV $[V_6O_{13}(TRIS^R)_2]^{2^-}$ ($R=CH_3$, CH_2CH_3 , CH_2OH , NO_2 , $N(CH_3)_2$), ligand substitution can tune the redox profile of the cluster by ~ 0.5 V. The minimal shifts in redox profiles of the TRIOL-functionalized Ti-POVs when compared to the unsubstituted complexes indicates that the functional groups are sufficiently decoupled from the hexametalate core, such that they do not influence the electrochemical properties of the system. This points to the fundamental differences in electrochemical properties between alkoxide-bridged POVs and primarily oxo-bridged scaffolds. In TRISR functionalized POV-alkoxides, there exist nine bridging alkoxide units in addition to the TRIOL group, and these moieties serve to provide additional stability and charge compensation to the mixed-valent core. In contrast, for compounds such as $[V_6O_{13}(TRIS^R)_2]^{2^-}$, which are supported only by two TRISR substituents, changes at "R" have a much more substantial influence on the electronics of the cluster.

CONCLUSION.

Here, we continue our work in expanding the POV-alkoxide family through the synthesis and characterization of four new heterometallic, TRIOL-functionalized clusters. We determine

that ligand identity has significant bearing on the self-assembly of the heterometallic core, with reducing substituents (i.e. pyridyl) favoring mono-titanium formation, while neutral groups (methyl, ethyl, and nitro) yield di-titanium clusters. Although functional group identity affects the assembly of these heterometallic clusters, it bears little influence on their electrochemical properties, further supporting our previous observations that significant modifications can be made at the peripheral ligands of POV-alkoxides without altering their multi-event redox profiles. ¹⁵⁻¹⁶ This work details new insights into the synthesis and electrochemical properties of functionalized, heterometallic POV-alkoxides, highlighting pathways for further development of POM-based organic-inorganic hybrids.

EXPERIMENTAL SECTION.

General Considerations.

Where specified, air- and moisture-sensitive manipulations were carried out in the absence of water and oxygen in a UniLab MBraun inert atmosphere glovebox under a dinitrogen atmosphere. Glassware was oven dried for a minimum of 4 hours and cooled in an evacuated antechamber prior to use in the glove box. Anhydrous methanol was purchased from Sigma-Aldrich and stored over activated 4 Å molecular sieves (Fisher Scientific). Acetonitrile (Fisher Chemical) used for electrochemical experiments was deoxygenated and dried on a Glass Contour System (Pure Process Technology, LLC) and stored over activated 4 Å molecular sieves (Fisher Scientific). All other solvents (dichloromethane and diethyl ether) were used as received outside the glove box without drying or degassing. [nBu4N][BH4], [Me4N][BH4], H3CC-(CH2OH)3 (TRISMe), H5C2C-(CH2OH)3 (TRISEt), iodomethane, and VO(OC2H5)3 were purchased from Sigma-Aldrich and used as received. O2NC-(CH2OH)3 (TRISNO2) was purchased from Oakwood Chemical and used as

received. Sodium carbonate (Macron Fine Chemicals) was used as received. [ⁿBu₄N][PF₆] was purchased from Sigma-Aldrich, recrystallized thrice using hot ethanol, and stored under dynamic vacuum for a minimum of two days prior to use. The ligand TRIS^{Py} [(C₅H₄N)-C(CH₂OH)₃] was synthesized according to literature procedures.²⁵ The details of the modifications to these synthetic procedures are summarized in the supporting information file.

Electronic absorption measurements were recorded at room temperature in sealed 1 cm quartz cuvettes with an Agilent Cary 60 UV-Vis spectrophotometer. All electrochemical experiments were conducted in the glove box using a Bio-Logic VMP3 potentiostat/galvanostat and the EC-Lab software suite. ¹H NMR spectra were recorded on a Bruker DPX-500 spectrometer at 11.7 Tesla while locked on to deuterated solvent. Deuterated CDCl₃ was purchased from Cambridge Isotope Laboratories and used as received from the manufacturer. A Shimadzu IRAffinity-1 Fourier Transform Infrared spectrophotometer was used to record all infrared spectra [FT-IR (ATR)] and are reported in wavenumbers (cm⁻¹). All mass spectrometry spectra were recorded on an Advion Expression^L Compact Mass Spectrometer equiped with an electrospray probe and ion-trap mass analyzer. All samples were analyzed by direct injection with the carrier solvent acetontrile. X-ray quality single crystals were mounted on a thin Nylon loop and positioned on a XtaLab Synergy-S Dualflex diffractometer equipped with a HyPix-6000He HPC area detector for data collection at 100.0(5) K. Structure solutions were obtained using SHELXT-2014/5²⁶ and refined using SHELXL-2014/7.²⁷ A PerkinElmer 2400 Series II Analyzer (CENTC Elemental Analysis Facility, University of Rochester) was used for elemental analyses.

In the glovebox, a 25 mL Teflon-lined autoclave (PARR) was charged with VO(OCH₃)₃ (0.250 g, 1.56 mmol), Ti(O'Pr)₄ (0.222 g, 0.78 mmol), H₃CC-(CH₂OH)₃ (0.094 g, 0.78 mmol), and methanol (10 mL). The steel reaction vessel was sealed, and the mixture heated to 125 °C for 48 hours. After the allotted time period, the autoclave was cooled to room temperature, and subsequent working completed in ambient atmosphere. The resulting deep red solution was reduced to half its original volume under reduced pressure, then left to stand at room temperature for at least 24 hours. After standing, several large spherulites were clearly observed in the bottom of the vial (Figure S5). The mother liquor was decanted, and these spheres washed with pentane (3x10mL) to give pure Ti₂V₄-TRIS^{Me} for characterization. Subsequent precipitations from the mother liquor were combined to improve the yield (0.137 g, 0.16 mmol, 42 %). ¹H NMR (500 MHz, CDCl₃): δ = -0.42 (br), 3.42 (s), 3.95 (s), 6.15 (br), 12.68 (br), 14.84 (br), 28.03 (br). IR (ATR, cm⁻¹): 972 (V=O), 1018 (O-CH₃), 1124 (Ti-OCH₃). UV-Vis [ε (M⁻¹ cm⁻¹)]: 386 nm (5.69 x 10²), 634 nm (5.3 x 10¹). EA Calcd. for C₁₆H₄₂O₁₉Ti₂V₄ (MW=838 g/mol): C, 22.93; H, 5.05. Found: C, 22.678; H, 4.592.

Preparation of $[Ti_2V_4O_5(OCH_3)_{11}(OCH_2)_3CC_2H_5]$ (Ti_2V_4 - $TRIS^{Et}$)

In the glovebox, a 25 mL Teflon-lined autoclave (PARR) was charged with VO(OCH₃)₃ (0.250 g, 1.56 mmol), Ti(O^fPr)₄ (0.222 g, 0.78 mmol), H₅C₂C-(CH₂OH)₃ (0.105 g, 0.78 mmol), and methanol (10 mL). The steel reaction vessel was sealed, and the mixture heated to 125 °C for 48 hours. After the allotted time period, the autoclave was cooled to room temperature, and subsequent working completed in ambient atmosphere. The resulting deep red solution was reduced to half its original volume under reduced pressure, then left to stand at room temperature for at least 24 hours. After standing, several large spherulites were observed in the bottom of the

vial. The mother liquor was decanted, and solids were washed with pentane (3x10mL) to give pure Ti_2V_4 - $TRIS^{Et}$ for characterization. Subsequent precipitations from the mother liquor were combined to improve the yield (0.170 g, 0.20 mmol, 51 %). X-ray quality crystals were obtained from a saturated MeOH solution cooled to -35 °C. 1 H NMR (500 MHz, CDCl₃): δ = -0.29 (br), 1.65 (s), 1.84 (s), 3.97 (s), 6.15 (br), 12.72 (br), 14.94 (br), 28.23 (br). IR (ATR, cm⁻¹): 974 (V=O), 1022 (O-CH₃), 1120 (Ti-OCH₃). UV-Vis [ε (M⁻¹ cm⁻¹)]: 386 nm (5.65 x 10²), 644 nm (5.9 x 10¹). EA Calcd. for $C_{17}H_{44}O_{19}Ti_2V_4$ (MW=852 g/mol): $C_{17}C_$

Preparation of $[Ti_2V_4O_5(OCH_3)_{11}(OCH_2)_3CNO_2]$ (Ti_2V_4 - $TRIS^{NO_2}$)

In the glovebox, a 25 mL Teflon-lined autoclave (PARR) was charged with VO(OCH₃)₃ (0.250 g, 1.56 mmol), Ti(O⁷Pr)₄ (0.222 g, 0.78 mmol), O₂NC-(CH₂OH)₃ (0.118 g, 0.78 mmol), and methanol (10 mL). The steel reaction vessel was sealed, and the mixture heated to 125 °C for 48 hours. After the allotted time period, the autoclave was cooled to room temperature, and subsequent working completed in ambient atmosphere. The resulting deep red solution was reduced to half its original volume under reduced pressure, then left to stand at room temperature for at least 24 hours. After standing, several large spherulites were clearly observed in the bottom of the vial. The mother liquor was decanted, and the remaining solids were washed with pentane (3x10mL) to give pure Ti_2V_4 - $TRIS^{NO_2}$ for characterization. Subsequent precipitations from the mother liquor were combined to improve the yield (0.160 g, 0.18 mmol, 47 %). X-ray quality crystals were obtained from slow evaporation of Et_2O/DCM . ¹H NMR (500 MHz, CDCl₃): δ = 1.71 (s), 3.33 (s), 3.95 (s), 5.58 (br), 6.22 (br), 12.89 (br), 15.98 (br), 28.76 (br). IR (ATR, cm⁻¹): 974 (V=O), 1013 (O-CH₃), 1088, 1124 (Ti-OCH₃), 1339, 1535 (C-N). UV-Vis [ε (M⁻¹ cm⁻¹)]: 425 nm (4.49 x 10²), 640 nm

 (6.1×10^{1}) . EA Calcd. for $C_{15}H_{39}NO_{21}Ti_{2}V_{4}$ (MW=869 g/mol): C, 20.73; H, 4.52; N, 1.61. Found: C, 20.582; H, 4.021; N, 1.471.

Preparation of $[TiV_5O_6(OCH_3)_{10}(OCH_2)_3CC_5H_4N]$ (TiV_5 - $TRIS^{Py}$)

In the glovebox, a 25 mL Teflon-lined autoclave (PARR) was charged with VO(OCH₃)₃ (0.250 g, 1.56 mmol), Ti(OⁱPr)₄ (0.088 g, 0.31 mmol), NH₄C₅C-(CH₂OH)₃ (0.057 g, 0.31 mmol), and methanol (10 mL). The steel reaction vessel was sealed, and the mixture heated to 100 °C for 24 hours. After the allotted time period, the autoclave was cooled to room temperature, and subsequent working completed in ambient atmosphere. The green-brown solution was condensed under reduced pressure to half its original volume, and left to stand overnight. A sticky green-brown precipitate formed, which was separated from the mother liquor to yield **TiV₅-TRIS**^{Py} (0.086 g, 0.09 mmol, 31 %). IR (ATR, cm⁻¹): 958 (V=O), 1036 (O-CH₃), 1162 (Ti-OCH₃). UV-Vis [ε (M⁻¹ cm⁻¹)]: 382 nm (4.29 x 10³), 656 nm (3.25 x 10²), 1000 nm (7.65 x 10²). EA Calcd. for C₁₉H₄₀NO₁₉TiV₅ (MW=890 g/mol): C, 25.67; H, 4.53; N, 1.58. Found: C, 25.601; H, 4.400; N, 1.438.

ACKNOWLEDGMENTS

The authors acknowledge Gabriel Martinez for his assistance in the characterization of the POV-alkoxides. The authors thank the University of Rochester for funding support. L. E. V. is supported by the National Science Foundation Graduate Research Fellowship Program (DGE-1419118).

REFERENCES

- 1. Zhang, J.; Huang, Y.; Li, G.; Wei, Y., Recent advances in alkoxylation chemistry of polyoxometalates: From synthetic strategies, structural overviews to functional applications. *Coord. Chem. Rev.* **2019**, *378*, 395-414.
- 2. Gumerova, N. I.; Rompel, A., Synthesis, structures and applications of electron-rich polyoxometalates. *Nat. Rev. Chem.* **2018**, *2*, 0112.
- 3. Pope, M. T.; Müller, A., Polyoxometalate Chemistry: An Old Field with New Dimensions in Several Disciplines. *Angew. Chem. Int. Ed.* **1991**, *30*, 34-48.
- 4. Gouzerh, P.; Proust, A., Main-Group Element, Organic, and Organometallic Derivatives of Polyoxometalates. *Chem. Rev.* **1998,** *98*, 77-112.
- 5. Proust, A.; Thouvenot, R.; Gouzerh, P., Functionalization of polyoxometalates: Towards advanced applications in catalysis and materials science. *Chem. Commun.* **2008**, 1837-1852.
- 6. Dolbecq, A.; Dumas, E.; Mayer, C. R.; Mialane, P., Hybrid organic-inorganic polyoxometalate compounds: From structural diversity to applications. *Chem. Rev.* **2010**, *110*, 6009-6048.
- 7. Long, D.-L.; Tsunashima, R.; Cronin, L., Polyoxometalates: Building Blocks for Functional Nanoscale Systems. *Angew. Chem. Int. Ed.* **2010**, *49*, 1736-1758.
- 8. Piepenbrink, M.; Triller, M. U.; Gorman, N. H. J.; Krebs, B., Bridging the Gap between Polyoxometalates and Classic Coordination Compounds: A Novel Type of Hexavanadate Complex. *Angew. Chem. Int. Ed.* **2002**, *41*, 2523-2525.
- 9. Chen, Q.; Goshorn, D. P.; Scholes, C. P.; Tan, X. L.; Zubieta, J., Coordination compounds of polyoxovanadates with a hexametalate core. Chemical and structural characterization of $[V^V_6O_{13}[(OCH_2)_3CR]_2]^{2-}$, $[V^V_6O_{11}(OH)_2[(OCH_2)_3CR]_2]$, $[V^{IV}_4V^V_2O_9(OH)_4[(OCH_2)_3CR]_2]^{2-}$, and $[V^{IV}_6O_7(OH)_6](OCH_2)_3CR]_2]^{2-}$. *J. Am. Chem. Soc.* **1992,** *114*, 4667-4681.
- 10. Daniel, C.; Hartl, H., Neutral and Cationic VIV/VV Mixed-Valence Alkoxopolyoxovanadium Clusters $[V_6O_7(OR)_{12}]^{n+}$ (R = -CH₃, -C₂H₅): Structural, Cyclovoltammetric and IR-Spectroscopic Investigations on Mixed Valency in a Hexanuclear Core. *J. Am. Chem. Soc.* **2005**, *127*, 13978-13987.
- 11. Khan, M. I.; Chen, Q.; Zubieta, J.; Goshorn, D. P., Hexavanadium polyoxoalkoxide anion clusters: structures of the mixed-valence species $(Me_3NH)[V^{IV}_5V^VO_7(OH)_3\{CH_3C(CH_2O)_3\}_3]$ and of the reduced complex $Na_2[V^{IV}_6O_7\{CH_3CH_2C(CH_2O)_3\}_4]$. *Inorg. Chem.* **1992**, *31*, 1556-1558.
- 12. Chen, Q.; Zubieta, J., Synthesis and structural characterization of a polyoxovanadate coordination complex with a hexametalate core: [(n-C₄H₉)₄N]₂[V₆O₁₃{O₂NC(CH₂O)₃}₂]. *Inorg. Chem.* **1990,** *29*, 1456-1458.
- 13. Spandl, J.; Daniel, C.; Brüdgam, I.; Hartl, H., Angew. Chem. Int. Ed. 2003, 42, 1163-1166.
- 14. Daniel, C.; Hartl, H., A Mixed-Valence V^{IV}/V^V Alkoxo-polyoxovanadium Cluster Series [V₆O₈(OCH₃)₁₁]^{n+/-}: Exploring the Influence of a μ-Oxo Ligand in a Spin Frustrated Structure. *J. Am. Chem. Soc.* **2009**, *131*, 5101-5114.
- 15. Schurr, B.; Nachtigall, O.; VanGelder, L. E.; Brennessel, W. W.; Matson, E. M., Synthesis and characterization of polar-functionalized polyoxovanadate-alkoxide clusters. *J. Coord. Chem.* **2019**, *Accepted Article* (DOI: 10.1080/00958972.2019.1595605).
- 16. VanGelder, L. E.; Petel, B. E.; Nachtigall, O.; Martinez, G.; Brennessel, W. W.; Matson, E. M., Organic Functionalization of Polyoxovanadate–Alkoxide Clusters: Improving the

- Solubility of Multimetallic Charge Carriers for Nonaqueous Redox Flow Batteries. *ChemSusChem* **2018**, *11*, 4139-4149.
- 17. Nachtigall, O.; Spandl, J., Versatile Organic Chemistry on Vanadium-Based Multi-Electron Reservoirs. *Chem. Eur. J.* **2018**, *24*, 2785-2789.
- 18. VanGelder, L. E.; Brennessel, W. W.; Matson, E. M., Tuning the redox profiles of polyoxovanadate-alkoxide clusters via heterometal installation: toward designer redox Reagents. *Dalton Trans.* **2018**, *47*, 3698-3704.
- 19. Li, F.; VanGelder, L. E.; Brennessel, W. W.; Matson, E. M., Self-Assembled, Iron-Functionalized Polyoxovanadate Alkoxide Clusters. *Inorg. Chem.* **2016**, *55*, 7332-7334.
- 20. Meyer, R. L.; Brennessel, W. W.; Matson, E. M., Synthesis of a gallium-functionalized polyoxovanadate-alkoxide cluster: Toward a general route for heterometal installation. *Polyhedron* **2018**, *156*, 303-311.
- 21. VanGelder, L. E.; Forrestel, P. L.; Brennessel, W. W.; Matson, E. M., Site-selectivity in the halogenation of titanium-functionalized polyoxovanadate—alkoxide clusters. *Chem. Commun.* **2018**, *54*, 6839-6842.
- 22. VanGelder, L. E.; Matson, Ellen M., Heterometal functionalization yields improved energy density for charge carriers in nonaqueous redox flow batteries. *J. Mat. Chem. A* **2018**, *6*, 13874-13882.
- 23. Li, F.; Carpenter, S. H.; Higgins, R. F.; Hitt, M. G.; Brennessel, W. W.; Ferrier, M. G.; Cary, S. K.; Lezama-Pacheco, J. S.; Wright, J. T.; Stein, B. W.; Shores, M. P.; Neidig, M. L.; Kozimor, S. A.; Matson, E. M., Polyoxovanadate–Alkoxide Clusters as a Redox Reservoir for Iron. *Inorg. Chem.* **2017**, *56*, 7065-7080.
- 24. VanGelder, L. E.; Kosswattaarachchi, A. M.; Forrestel, P. L.; Cook, T. R.; Matson, E. M., Polyoxovanadate-alkoxide clusters as multi-electron charge carriers for symmetric non-aqueous redox flow batteries. *Chem. Sci.* **2018**, *9*, 1692-1699.
- 25. Menozzi, D.; Biavardi, E.; Massera, C.; Schmidtchen, F.-P.; Cornia, A.; Dalcanale, E., Thermodynamics of host-guest interactions between methylpyridinium salts and phosphonate cavitands. *Supramol. Chem.* **2010**, *22*, 768-775.
- 26. Sheldrick, G., SHELXT-2014/5.
- 27. Sheldrick, G., Crystal structure refinement with SHELXL. *Acta Cryst. C* **2015**, *71*, 3-8.